High-Contrast PET Imaging of Vasopressin V_{1B} Receptors with a Novel Radioligand, ^{11}C-TASP699

Kazumi Koga[1,2], Yuji Nagai[1], Masayuki Hanyu[1], Mitsukane Yoshinaga[2], Shigeyuki Chaki[2], Norikazu Ohtake[2], Satoshi Ozaki[2], Ming-Rong Zhang[1], Tetsuya Suhara[1], and Makoto Higuchi[1]

[1]National Institute of Radiological Sciences, National Institutes for Quantum and Radiological Science and Technology, Chiba, Japan; and [2]Taisho Pharmaceutical Co., Ltd., Saitama, Japan

Vasopressin 1B receptors (V_{1B}Rs) are abundantly expressed in the pituitary, and in vivo PET of V_{1B}Rs was recently enabled by our development of a specific radioligand, ^{11}C-TASP0434299, derivatized from pyridopyrimidin-4-one. Here, we identified a novel pyridopyrimidin-4-one analog, *N-tert*-butyl-2-[2-(6-^{11}C-methoxypyridine-2-yl)-6-[3-(morpholin-4-yl)propoxy]-4-oxopyrido[2,3-*d*]pyrimidin-3(4*H*)-yl]acetamide (^{11}C-TASP0410699, hereafter referred to as ^{11}C-TASP699), as a potent V_{1B}R radioligand producing a higher image contrast for the target than ^{11}C-TASP0434299. **Methods:** In vitro properties of TASP699 were assessed by assaying its affinity for human V_{1B}R and its selectivity for off-target molecules. Radioactive uptake in the pituitary was analyzed using PET in rhesus monkeys after intravenous administration of ^{11}C-TASP699. Serial doses of a selective V_{1B}R antagonist, 2-[2-(3-chloro-4-fluorophenyl)-6-[3-(morpholin-4-yl)propoxy]-4-oxopyrido[2,3-*d*]pyrimidin-3(4*H*)-yl]-*N*-isopropylacetamide hydrochloride (TASP0390325), were administered before the radioligand injection. Autoradiographic labeling of monkey pituitary slices with ^{11}C-TASP699 was conducted with or without nonradioactive V_{1B}R antagonists. **Results:** The half maximal inhibitory concentration (IC_{50}) of TASP699 for human V_{1B}Rs (0.165 nM) was lower than that of TASP0434299 (0.526 nM), whereas its IC_{50} values for off-target molecules exceeded 1 μM. PET imaging in monkeys demonstrated that the peak pituitary uptake of ^{11}C-TASP699 was almost equivalent to that of ^{11}C-TASP0434299 and that pretreatment with TASP0390325 inhibited the retention of ^{11}C-TASP699 in a dose-dependent manner, inducing nearly full occupancy at 0.3 mg/kg. Specific radioligand binding was determined as a specific–to–nondisplaceable uptake ratio at equilibrium using radioactivity retentions at 60 min in baseline and blocking studies. This ratio for ^{11}C-TASP699 was approximately 2.5-fold greater than that of ^{11}C-TASP0434299. A reversed-phase high-performance liquid chromatography study identified the parent and polar radiometabolites. Affinities of 2 predicted metabolite candidates for V_{1B}Rs were more than 10 times weaker than that of the parent. Intense autoradiographic labeling of the anterior pituitary with ^{11}C-TASP699 was inhibited with TASP0390325 in a concentration-dependent manner. **Conclusion:** ^{11}C-TASP699 yielded PET images of pituitary V_{1B}Rs with a higher contrast than ^{11}C-TASP0434299, supporting the applicability of ^{11}C-TASP699 in the assessment of neuropsychiatric diseases and dose findings for test drugs in clinical trials.

Key Words: vasopressin; V_{1B} receptor; pituitary; positron emission tomography

J Nucl Med 2017; 58:1652–1658
DOI: 10.2967/jnumed.116.188698

Arginine vasopressin (AVP) is an endogenous cyclic nonapeptide that is mainly synthesized in the hypothalamus and is involved in diverse physiologic functions, which are triggered by the activation vasopressin 1A (V_{1A}), 1B, and 2 (V_2) receptors and oxytocin receptors (*1–5*).

Of these, the V_{1B} receptor (V_{1B}R) is expressed abundantly in the anterior pituitary (*6–8*), and its activation leads to the secretion of adrenocorticotropic hormones from corticotrophs, which play a pivotal role in stress responses through the modulation of the hypothalamic–pituitary–adrenal axis (*9,10*). V_{1B}R antagonists have been reported to show pharmacologic actions in animal models (*11–14*), whereas the effectiveness of V_{1B}R antagonists in humans has yet to be clarified (*15,16*). It is accordingly required to demonstrate and quantify the target engagement of test compounds to the V_{1B}R to determine appropriate doses for clinical efficacy. For this purpose, an imaging agent allowing measurements of the density and occupancy of V_{1B}Rs in living animal models and humans is essential.

Recently, we documented the use of a pyridopyrimidin-4-one derivative, *N-tert*-butyl-2-[2-(3-methoxyphenyl)-6-[3-(morpholin-4-yl)propoxy]-4-oxopyrido[2,3-*d*]pyrimidin-3(4*H*)-yl]acetamide (TASP0434299, Fig. 1), radiolabeled with ^{11}C for the visualization of V_{1B}Rs in the monkey pituitary (*17*). Because this compound was a prototypical agent in this structural class, the possibility of developing an analog capable of capturing V_{1B}Rs with a larger dynamic range remained to be explored.

Here, we screened our library of pyridopyrimidin-4-one derivatives for a compound with a higher affinity for V_{1B}Rs than TASP0434299 and found a novel analog, TASP699 (Fig. 1), to have a sufficient potency and selectivity. In a subsequent monkey PET study, ^{11}C-TASP699 produced a contrast for pituitary V_{1B}Rs superior to that of ^{11}C-TASP0434299. Moreover, the utility of ^{11}C-TASP699 for measuring the occupancy of V_{1B}Rs was supported by a reduction in radioligand retention in a manner dependent on the pretreatment dose of a selective V_{1B}R antagonist, TASP0390325, which has been well characterized in studies on behavioral pharmacology and receptor occupancy (*14,17*).

Received Dec. 16, 2016; revision accepted Apr. 13, 2017.
For correspondence or reprints contact: Makoto Higuchi, Department of Functional Brain Imaging Research, National Institute of Radiological Sciences, National Institutes for Quantum and Radiological Science and Technology, 4-9-1 Anagawa, Inage-ku, Chiba 263-8555, Japan.
E-mail: higuchi.makoto@qst.go.jp
Published online Apr. 27, 2017.

MATERIALS AND METHODS

Animals

Two male rhesus monkeys (*Macaca mulatta*) weighing 5.2–6.5 kg were housed under a 14-h light/10-h dark cycle (lights on at 7:00 AM) in a temperature- and humidity-controlled holding room, with food and water available ad libitum. All the PET experiments using monkeys were approved by the Committee for the Care and Use of Laboratory Animals of the National Institutes for Quantum and Radiologic Science and Technology and were performed in accordance with the ethical standards of the Institutes.

Drugs

TASP699, TASP0434299, and their desmethyl precursors for ^{11}C radiolabeling were synthesized at Taisho Chemistry Laboratories, as described in a previous patent application (*18*). TASP0390325 and (4*R*)-1-[5-chloro-1-[(2,4-dimethoxyphenyl)sulfonyl]-3-(2-methoxyphenyl)-2-oxo-2,3-dihydro-1*H*-indol-3-yl]-4-fluoro-*N*,*N*-dimethyl-L-prolinamide (levorotatory isomer) (TASP0233278), 3-({3-[2-(*tert*-butylamino)-2-oxoethyl]-2-(6-methoxypyridin-2-yl)-4-oxo-3,4-dihydropyrido[2,3-*d*]pyrimidin-6-yl}oxy)propanoic acid (candidate TASP699 metabolite 1), and *N*-*tert*-butyl-2-[6-{3-[(2-hydroxyethyl)amino]propoxy}-2-(6-methoxypyridin-2-yl)-4-oxopyrido[2,3-*d*]pyrimidin-3(4*H*)-yl]acetamide (candidate TASP699 metabolite 2) were synthesized at Taisho Chemistry Laboratories. AVP was purchased from Sigma-Aldrich. Oxytocin was purchased from Peptide Institute, Inc. Vasopressin (8-L-arginine), [phenylalanyl-3,4,5-^{3}H(N)] (^{3}H-AVP), and oxytocin, [tyrosyl-2, 6-^{3}H] (^{3}H-oxytocin) were purchased from PerkinElmer.

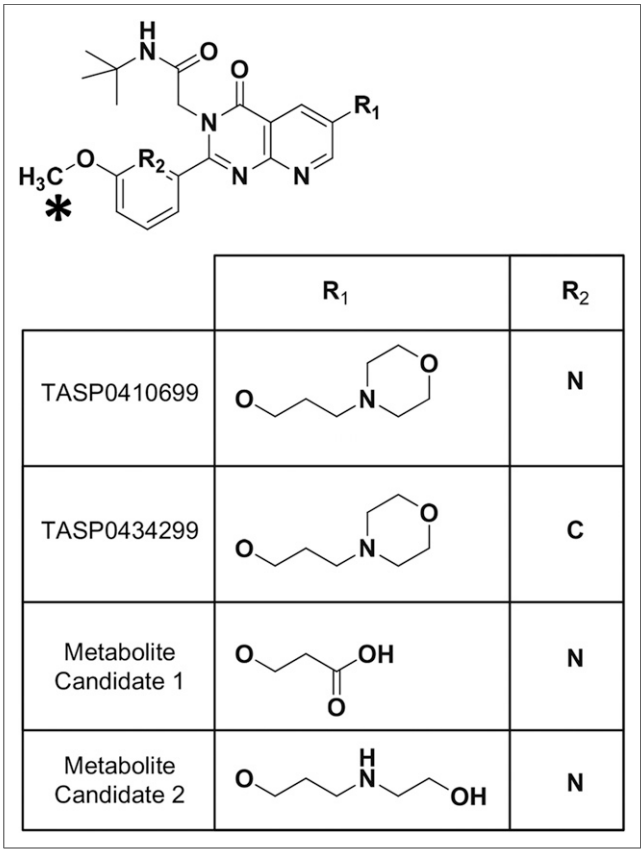

FIGURE 1. Chemical structures of radioligands and candidate metabolites of TASP699. * = methoxy moiety to be radiolabeled with ^{11}C.

Partition Coefficient

The calculated partition coefficient of the compounds was determined using software from Daylight Chemical Information Systems.

Receptor Binding Assays

Radioligand Binding to Human V_{1A}, V_{1B}, V_2, and Oxytocin Receptors. Membranes were prepared from 293FT cells expressing human V_{1B}Rs. Membranes of 1321-N1 cells expressing human V_{1A} and V_2 receptors were purchased from PerkinElmer. Membranes of Chem-1 cells expressing oxytocin receptors were purchased from Eurofins Pharma Bioanalytics Services US, Inc. ^{3}H-AVP binding to membranes expressing human V_{1A}, V_{1B}, or V_2 receptors and ^{3}H-oxytocin binding to membranes expressing human oxytocin receptors were performed as previously reported (*17*). The assays were performed 3–6 times, and each test was performed in duplicate.

Binding Selectivity of TASP699. The binding of 1 μM of TASP699 to 87 off-target molecules, including adenosine A_1, A_{2a}, and A_3; adrenergic α_{1A}, α_{1B}, α_{2A}, α_{2B}, α_{2C}, β_1, and β_2; angiotensin AT_1 and AT_2; bradykinin B_1 and B_2; bombesin; cannabinoid CB_1 and CB_2; cholecystokinin A and B; corticotropin-releasing factor 1; dopamine D_1, D_2, D_3, $D_{4.2}$, and D_5; endothelin ET_A and ET_B; γ-aminobutanoic acid B; histamine H_1, H_2, and H_3; leukotriene B_4 and D_4; melatonin MT_1; muscarinic M_1, M_2, M_3, M_4, and M_5; neurokinin NK_1, NK_2, and NK_3; neuropeptide Y_1 and Y_2; neurotensin NT_1; opiate μ, δ, κ, and opioid receptorlike 1; platelet-activating factor; prostanoid EP_2; serotonin 1A and 2A; vasoactive intestinal peptide 1; androgen; estrogen; glucocorticoid; imidazoline; σ-σ_1 and σ_2 receptors and Na^+ channel site 2; K^+ channel (K_A, K_{ATP}, SK_{Ca}); Ca^{2+} channel (type L [benzothiazepine, dihydropyridine, and phenylalkylamine] and type N); γ-aminobutanoic acid A (agonist site, benzodiazepine site, and chloride channel); glutamate (2-amino-3-(3-hydroxy-5-methyl-isoxazol-4-yl)propanoic acid, kainite, *N*-methyl-D-aspartate agonist site, *N*-methyl-D-aspartate glycine site, *N*-methyl-D-aspartate phencyclidine site, and *N*-methyl-D-aspartate polyamine site); glycine (strychnine-sensitive); nicotinic acetylcholine receptor; serotonin 3 receptor; inositol 1,4,5-trisphosphate receptor; and adenosine, dopamine, γ-aminobutanoic acid, monoamine, norepinephrine, and serotonin transporters, were evaluated at Sekisui Medical.

Antagonistic Activity at Human V_{1B}R

Chinese hamster ovary K_1 cells stably expressing human V_{1B}R were used for quantifying inhibitions of an AVP-induced increase of an intracellular calcium concentration ($[Ca^{2+}]_i$) by TASP699, as described previously (*14,17*).

In Vitro Data Analysis

Concentration–response curves for in vitro receptor binding were generated by fitting a nonlinear regression to the experimental data. The half maximal inhibitory concentration (IC_{50}) was calculated using GraphPad Prism software (GraphPad Software Inc.). Estimates were expressed as the geometric mean of the IC_{50} values.

Synthesis of ^{11}C-Labeled Radioligands

^{11}C-CH_3I was produced as described previously (*19*). ^{11}C-CH_3I, the desmethyl precursor of TASP699 (1 mg), and K_2CO_3 (10 mg) were mixed in 300 μL of *N*,*N*-dimethylformamide at −10 to −15°C, then heated at 100°C for 3 min. Acetonitrile/50 mM phosphoric acid (1:4) solution (1 mL) was then added to the reaction mixture. Synthesized ^{11}C-TASP699 was purified using high-performance liquid chromatography (HPLC) (JASCO) with a SunFire C18 column (10-mm inner diameter × 250 mm; Waters) and a mobile phase consisting of an acetonitrile/50 mM phosphoric acid (1:4) solution at a flow rate of 5 mL/min. The eluent was monitored using an ultraviolet detector (JASCO) at a wave length of 300 nm and a NaI(TI) scintillation detector system (Ohyo Koken Kogyo). A fraction corresponding to ^{11}C-TASP699, the retention time of which was approximately 11 min,

was collected into a rotary evaporator flask containing 100 μL of polysorbate 80/ethanol (1:4) and 100 μL of 25% ascorbic acid. The solvent was removed in vacuo at 150°C, and the resulting residue was dissolved in 5 mL of 0.2 M sodium phosphate solution. The final products showed a radiochemical purity of greater than 98.5% and a specific activity of 93 ± 18 GBq/μmol (mean ± SD, $n = 10$). The average time for the radiosynthesis of ^{11}C-TASP699 from bombardment to the preparation of the injection solution was 30 min.

^{11}C-TASP0434299 was synthesized as described previously (*17*). The final products showed a radiochemical purity of greater than 99% and a specific activity of 56 ± 30 GBq/μmol (mean ± SD, $n = 3$).

PET Imaging of Anesthetized Monkeys Using ^{11}C-TASP0434299 and ^{11}C-TASP699

PET scans of monkeys were obtained as described previously (*17*). Emission scanning was conducted immediately after the intravenous injection of ^{11}C-TASP0434299 (injected radioactivity, 406 ± 55 MBq [range, 361–467 MBq]; mass dose, 6.1 ± 3.4 μg [range, 2.9–10 μg]; $n = 3$) or ^{11}C-TASP699 (injected radioactivity, 356 ± 26 MBq [range, 303–381 MBq]; mass dose, 2.7 ± 0.98 μg [range, 2.9–8.7 μg]; $n = 8$).

To examine the specific binding of ^{11}C-TASP699 to V_{1B}R, TASP0390325 was injected intravenously at doses of 0.01, 0.025, 0.3, 1, and 10.7 mg/kg at 10 min before radioligand injection. Blood (1–3 mL) was collected from the femoral vein at 5, 15, 30, 60, and 90 min after the injection of ^{11}C-TASP699 to determine venous plasma radioactivity.

Blood Analysis

Venous plasma was protein-precipitated and then used to analyze the parent and radiometabolites using HPLC (JASCO) as described elsewhere (*17*), with the exception that the flow rate of the mobile phase, consisting of 10 mM of ammonium acetate/acetonitrile (64:36), was 4 mL/min. The rate of radioactivity recovery in the supernatants after protein precipitation was 93% ± 3% (mean ± SD, $n = 28$). The fraction of the parent radioligand in the plasma was determined by calculating the ratio of the parent peak area versus all other peak areas in a radio-HPLC chart.

PET Image Data Analysis

Regions of interest were placed on the pituitary, whole brain, and temporal muscle using PMOD software (version 3.206; PMOD Technologies), with reference to individual MRI data. The tissue time–activity curve for each region of interest was generated by calculating the SUV in each time frame as follows:

$$\text{SUV} = \text{tissue radioactivity (Bq/g)} \times \text{body weight (g)} / \text{injected radiotracer dose (Bq)}.$$

The plasma radioactivity for the parent was determined using the time course data for plasma radioactivity and the fraction of the parent corrected for decay.

Autoradiography of Monkey Pituitary Slices with ^{11}C-TASP699

Autoradiography was performed as described elsewhere (*17*), with the exception that 3 nM of ^{11}C-TASP699 was used as a radioligand. The radioactivity retained on the sections was determined using an imaging plate and Typhoon FLA 7000 (GE Healthcare) after 2 h of exposure. The monkey pituitary slices were incubated in the presence of 0.1, 1, 10, and 10,000 nM of TASP0390325 or 1, 10, and 10,000 nM of TASP0233278. Regions of interest were placed on autoradiographic images of the anterior pituitary using ImageQuant TL (GE Healthcare). Radioactive signals were expressed as the percentage of the results obtained without any blocking agent. The IC_{50} value of TASP0390325 was calculated by fitting a nonlinear regression model to concentration–response data using GraphPad Prism software.

RESULTS

In Vitro Profiles of TASP699

The IC_{50} value of TASP699 for human V_{1B}Rs was approximately 3 times higher than that of TASP0434299 (Table 1). TASP699 more potently inhibited increases in $[Ca^{2+}]_i$ induced by 1 nM of AVP than TASP043299 (Table 1; Supplemental Fig. 1 [supplemental materials are available at http://jnm.snmjournals.org]).

In contrast, TASP699 did not show apparent binding affinities for other vasopressin receptor subtypes including V_{1A}, V_2, and oxytocin receptors, even at 10 μM (Table 1). Moreover, the IC_{50} of TASP699 for 87 other off-target molecules exceeded 1 μM (Supplemental Table 1).

Uptake of ^{11}C-TASP699 and ^{11}C-TASP0434299 in Pituitary Assessed by PET Imaging of Rhesus Monkeys

^{11}C-TASP699 displayed a slightly higher peak uptake in the pituitary followed by a slower clearance than ^{11}C-TASP0434299 in PET scans of the same rhesus monkey (Figs. 2A and 2B). The

TABLE 1
In Vitro Profiles of TASP699, TASP0434299, and Candidate Metabolites of TASP699

Compound/peptide	^{3}H-AVP binding: Human V_{1B} receptor	^{3}H-AVP binding: Human V_{1A} receptor	^{3}H-AVP binding: Human V_2 receptor	^{3}H-oxytocin binding, human oxytocin receptor	$[Ca^{2+}]_i$ assay, human V_{1B} receptor
TASP699	0.165	>10,000	>10,000	>10,000	0.381
Metabolite candidate 1	>1,000	—	—	—	—
Metabolite candidate 2	1.87	—	—	—	—
TASP0434299	0.526	>10,000	>10,000	>10,000	0.639
AVP	0.776	0.440	1.24	—	—
Oxytocin	—	—	—	0.731	—

— = not determined.
IC_{50} values (nM) are expressed as geometric means ($n = 3$–6).

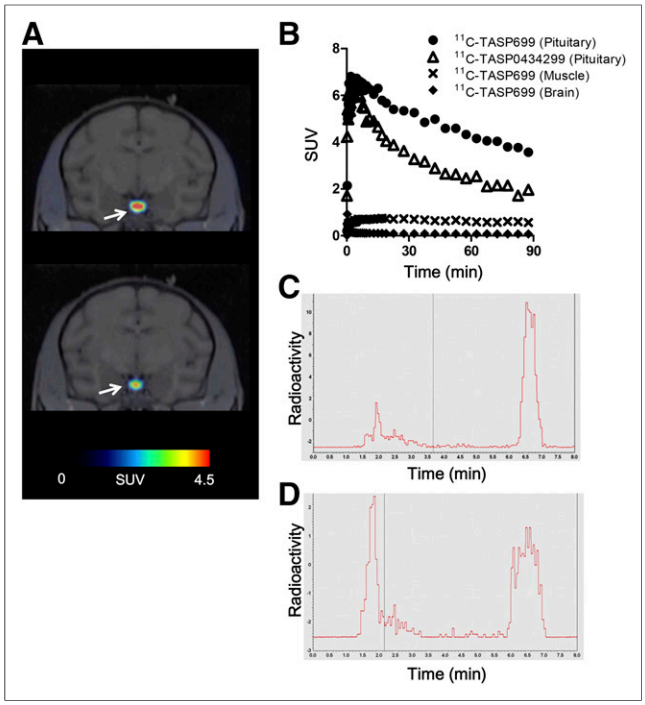

FIGURE 2. PET images of the head of an isoflurane-anesthetized rhesus monkey after intravenous injection of radioligands. (A) Representative coronal PET images after injection of ^{11}C-TASP699 (top) and ^{11}C-TASP0434299 (bottom). Images were averaged at 30–90 min after radioligand administration and were coregistered with cranial MR image of same monkey. Arrows indicate pituitary. (B) Representative time–radioactivity curve in pituitary (filled circles), temporal muscle (crosses), and whole brain (filled rhombi) after injection of ^{11}C-TASP699, and in pituitary after injection of ^{11}C-TASP0434299 (open triangles). (C and D) Representative reversed-phase high-performance liquid chromatograms of protein-precipitated plasma samples at 30 (C) and 60 (D) min after injection of ^{11}C-TASP699. Injection volumes of supernatant into HPLC were 0.43 mL (C) and 0.95 mL (D).

SUVs for ^{11}C-TASP699 and ^{11}C-TASP0434299 in the pituitary at 90 min after the injection were approximately 3.6 and approximately 2.0, respectively (Fig. 2B). The radioactivity uptake and retention in peripheral tissues lacking V_{1B}Rs represented by the temporal muscle were much lower than the pituitary values, and even lower and almost negligible radioactivity was observed in the brain (Fig. 2B).

A peak for unmetabolized ^{11}C-TASP699, with a retention time at 6–7 min, along with broad peaks for radiometabolites with a retention time at 1.5–3.5 min, were present in plasma collected at 30 and 60 min after radioligand injection (Figs. 2C and 2D). The fractions of the parent as determined as percentages of the total radioactive peak areas with radioactive decay corrections were 57% and 33% in monkeys 1 and 2, respectively, at 90 min after radioligand injection.

Two chemicals shown as candidates 1 and 2 (Fig. 1) were presumed to be potential metabolites of TASP699, which existed in the above-mentioned broad peaks, according to our preliminary in vitro assays of metabolites of unlabeled TASP699 after incubation with monkey liver microsomes (data not shown). The calculated partition coefficient values of TASP699 and metabolite candidates 1 and 2 were 1.68, −1.94, and −0.7, respectively. Metabolite candidate 1 showed no significant binding affinity for human V_{1B}Rs, whereas metabolite candidate 2 exhibited an affinity that was approximately 10 times lower than that of TASP699 (Table 1). Taken together, these data suggested minimal interactions among the radiometabolites of ^{11}C-TASP699 with V_{1B}Rs in PET imaging in monkeys.

The radioactive uptake in the monkey pituitary were dose-dependently inhibited by pretreatment with TASP0390325. Pretreatment with 0.3 mg/kg of TASP0390325 almost completely inhibited the specific binding of ^{11}C-TASP699, because the retention of radioactive signals in this pretreatment experiment was nearly equivalent to the level after pretreatment with 10.7 mg/kg of TASP0390325 (Fig. 3A). A similar suppression of radioligand retention was noted when the animal was pretreated with 10 mg/kg of unlabeled TASP699 (data not shown). The inhibition of radioligand binding by TASP0390325 in a dose-dependent manner was also observed in the other monkey, with similar levels of radioactive retention under maximal blockade observed in the 2 monkeys (Figs. 3A and 3B).

A small variability in the venous plasma radioactivity of the parent was found among the baseline and pretreatment experiments (Figs. 3C and 3D), but this variability was not associated with the dose of TASP0390325 (Figs. 3C and 3D), indicating that the reduction in radioactive uptake in the pituitary by pretreatment with TASP0390325 was unrelated to changes in the plasma levels of ^{11}C-TASP699.

Autoradiography of ^{11}C-TASP699 Binding Using Monkey Pituitary Slices

Binding of ^{11}C-TASP699 to monkey pituitary slices was specifically localized to the anterior lobe and was not detectable in the posterior lobe (Fig. 4A). The radioligand binding was inhibited by TASP0390325 in a concentration-dependent manner (Fig. 4B). The IC_{50} value of TASP0390325 was 2.16 nM (Fig. 4B). Similarly, a pilot assay indicated that binding of ^{11}C-TASP699 was blocked by TASP0233278, a V_{1B}R antagonist with a scaffold structure distinct from that of TASP0390325 (*14*).

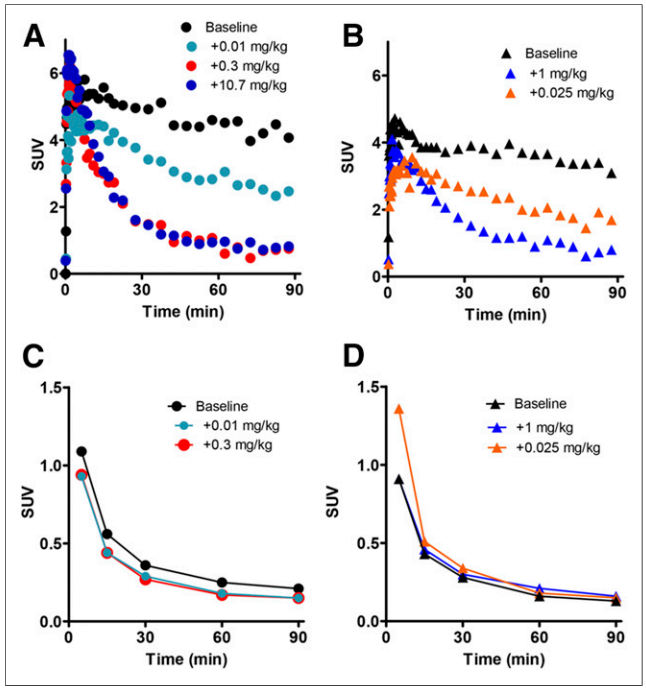

FIGURE 3. (A and B) Time–activity curves in pituitary and plasma of monkeys 1 (A) and 2 (B) after intravenous injection of ^{11}C-TASP699 with or without pretreatment with TASP0390325. (C and D) Time course of venous plasma radioactivity originating from parent in monkeys 1 (C) and 2 (D).

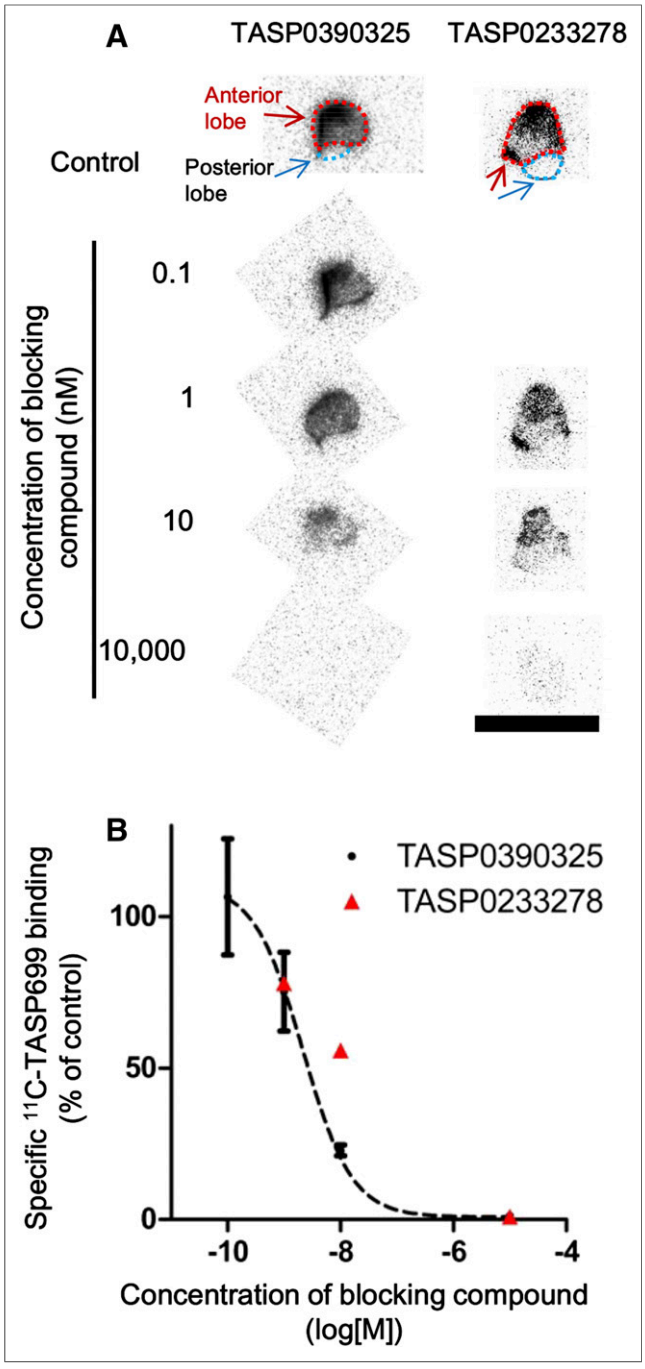

FIGURE 4. Autoradiographic labeling of pituitary slices prepared from rhesus monkey with ^{11}C-TASP699. (A) Representative images of pituitary samples autoradiographically labeled with ^{11}C-TASP699 without blockade (control) or with decreasing concentrations of TASP0390325 and of TASP0233278. Scale bar = 10 mm. (B) Specific binding of ^{11}C-TASP699 to slices inhibited by TASP0390325 (n = 3 in each condition) and TASP0233278 (n = 1 in each condition) in concentration-dependent fashion. Error bars for TASP0390325 data represent SEM.

DISCUSSION

Our previous work demonstrated the utility of ^{11}C-TASP0434299 for the visualization of V_{1B}Rs in monkey pituitary (*17*). Meanwhile, its relatively fast clearance from the target tissue suggested the possibility that structural modifications might enable the development of a radioligand with a higher contrast for V_{1B}Rs (*17*). In the present study, TASP699 was selected from our library of pyridopyrimidin-4-one derivatives as a potential radioligand with a 3-fold-higher affinity for V_{1B}Rs than TASP0434299. In addition, TASP699 showed a high selectivity for V_{1B}Rs over 90 off-target molecules including V_{1A}, V_2, and oxytocin receptors.

The in vivo PET findings in rhesus monkeys also supported the view that ^{11}C-TASP699 offers a greater dynamic range in the measurement of pituitary V_{1B}Rs than ^{11}C-TASP0434299. We estimated specific radioligand binding as a specific–to–nondisplaceable uptake ratio at equilibrium by calculating (ratio of radioactivity retention at 60 min between baseline and full blockade studies) minus 1.0. The specific binding determined by this method was approximately 4.0 for ^{11}C-TASP699 PET, which was nearly 2.5-fold greater than that for ^{11}C-TASP0434299 (*17*). Meanwhile, the uptake of ^{11}C-TASP699 in the monkey brain was low, and this was attributable to the property of TASP699 as a substrate for an efflux transporter, P-glycoprotein. Indeed, an efflux ratio for TASP699 quantified by an in vitro cell-based assay as described elsewhere (*17*) was 28.9, and was comparable to that of TASP0434299 (*17*). V_{1B}Rs in the rodent brain have been indicated by the presence of V_{1B}R messenger RNA and binding sites for a receptor ligand (*20,21*), and may play significant roles in central behaviors and functions, according to studies on knock-out mice (*22*). However, ^{11}C-TASP699 PET does not enable visualization of V_{1B}Rs in the intracranial structures except the pituitary. In this consideration, we did not determine whether ^{11}C-TASP699 can detect V_{1B}R in rhesus monkey brain slices by autoradiography. The low entry of ^{11}C-TASP699 into the brain also impedes the use of this organ as a reference tissue in a radioligand kinetic analysis without an arterial input function.

We also examined the applicability of ^{11}C-TASP699 to PET measurements of pituitary V_{1B}Rs with reference to plasma data. The present reversed-phase HPLC condition allowed us to identify the parent peak in the plasma, whereas some radiometabolites were not clearly separated from each other, presumably because of their polar physicochemical properties and excess volumes of injected samples (>0.4 mL) into HPLC.

The radiometabolites of ^{11}C-TASP699 in plasma include at least 2 chemicals, which were identified as in vitro metabolites of unlabeled TASP699 with monkey liver microsomes. The polarity of radiometabolites might be higher than that of the parent, according to the HPLC retention times, and this finding was consistent with the candidate metabolites having lower calculated partition coefficients than the parent.

On the basis of their binding affinity for V_{1B}Rs and their relative abundance in plasma, metabolite candidates 1 and 2 should not contribute to the radioactivity at specific binding sites profoundly. However, for more accurate assessments of the effects of metabolite candidates on the volume of distribution (*23*), it is required to improve the present HPLC conditions such as the use of column-switching HPLC to separate each radiometabolite (*24*).

The application of a V_{1B}R antagonist, TASP0390325, also supported the specificity of ^{11}C-TASP699 for V_{1B}Rs and the applicability of ^{11}C-TASP699 PET for estimating the receptor occupancies. TASP0390325 inhibited the pituitary retention of ^{11}C-TASP699 consistently in 2 monkeys in a dose-dependent manner. The intravenous injection of TASP0390325 at a dose of 0.3 mg/kg

induced full receptor occupancy without any significant effect on the plasma ^{11}C-TASP699 level. In addition, the in vitro autoradiographic binding of ^{11}C-TASP699 to pituitary slices was attenuated by TASP0390325, and its IC_{50} value was almost equivalent to those in a previous report (*14*).

Orally administered TASP0390325 (0.3 mg/kg) was previously reported to exert an antidepressant effect in rat models (*14*) and induced an approximately 50% receptor occupancy in the rat pituitary (*17*). Given that a 50% occupancy of pituitary V_{1B}Rs is required for a pharmacologic effect, the plasma concentration of a potential therapeutic agent acting on V_{1B}Rs and inducing a 50% occupancy can be determined in vivo in monkeys and then in humans by ^{11}C-TASP699 PET; such data would be useful for estimating a clinically relevant dose of a drug candidate.

The autoradiographic binding of ^{11}C-TASP699 to monkey pituitary slices was blocked by TASP0390325 and TASP0233278. TASP0390325 is a pyridopyrimidin-4-one derivative, and its interference with ^{11}C-TASP699 binding was predicted on a structural basis. Unlike these chemicals, TASP0233278 has an indolin-2-one core structure and is structurally similar to SSR149415 (*12*), a V_{1B}R antagonist that has been examined in clinical trials (*15*). Although the development of SSR149415 has been halted, our results justify the use of ^{11}C-TASP699 PET for in vivo assessments of the relationships between receptor occupancies by SSR149415 at clinically applied doses and its pharmacologic effects. Moreover, PET with ^{11}C-TASP699 would permit the quantification of V_{1B}R occupancy by other classes of chemicals including ABT-436, which has also been tested in clinical trials, notwithstanding that its chemical structure is yet to be disclosed (*16,25*).

^{11}C-TASP699 PET would also facilitate assessments of possible changes in the pituitary receptor binding under psychiatric conditions. Although there have been hitherto no demonstrations of altered V_{1B}R levels in patients with mental illnesses, rodent stress models were shown to display changes in the binding of ^{3}H-AVP to the pituitary (*26*). PET with ^{11}C-TASP699 would accordingly serve for selection of patient subsets with dysregulated V_{1B}R levels in the pituitary as candidates for therapies targeting these receptors.

CONCLUSION

We developed ^{11}C-TASP699 as a PET radioligand enabling the visualization of pituitary V_{1B}Rs with a higher contrast than the prototypical imaging agent, ^{11}C-TASP0434299. ^{11}C-TASP699 PET will offer an imaging-based biomarker for evaluations of hypothalamic–pituitary–adrenal axis activity and its alterations in psychiatric disorders. The estimation of V_{1B}R occupancies by a test drug using PET with ^{11}C-TASP699 will also facilitate the determination and prediction of effective drug dosages in nonclinical and clinical development stages.

DISCLOSURE

This study was funded by Taisho Pharmaceutical Co., Ltd. This study was supported in part by the Brain Mapping by Integrated Neurotechnologies for Disease Studies (to Tetsuya Suhara and Makoto Higuchi) and the Strategic Research Program for Brain Sciences (to Tetsuya Suhara) from the Japan Agency for Medical Research and Development and by Grants-in-Aid for Scientific Research on Innovative Areas ("Brain Environment") (23111009) (to Makoto Higuchi) from the Ministry of Education, Culture, Sports, Science and Technology, Japan. Kazumi Koga, Mitsukane Yoshinaga, Shigeyuki Chaki, Norikazu Ohtake, and Satoshi Ozaki are full-time employees of Taisho Pharmaceutical Co., Ltd. Kazumi Koga, Masayuki Hanyu, Mitsukane Yoshinaga, Ming-Rong Zhang, Tetsuya Suhara, and Makoto Higuchi hold a patent for ^{11}C-TASP699 and related chemicals as V_{1B}R ligands (Japan patent JP2015-120644A). No other potential conflict of interest relevant to this article was reported.

ACKNOWLEDGMENTS

We thank Dr. Akiko Yasuhira, Yasunori Kawakita, and Takuya Ichikawa for providing the in vitro data on candidate metabolites of TASP699 using monkey liver microsomes, and the staff of the Department of Radiopharmaceuticals Development, National Institutes for Quantum and Radiological Science and Technology, for their support with the radiosynthesis.

REFERENCES

1. Koshimizu TA, Nakamura K, Egashira N, Hiroyama M, Nonoguchi H, Tanoue A. Vasopressin V_{1a} and V_{1b} receptors: from molecules to physiological systems. *Physiol Rev.* 2012;92:1813–1864.
2. Thibonnier M, Auzan C, Madhun Z, Wilkins P, Berti-Mattera L, Clauser E. Molecular cloning, sequencing, and functional expression of a cDNA encoding the human V_{1a} vasopressin receptor. *J Biol Chem.* 1994;269:3304–3310.
3. Sugimoto T, Saito M, Mochizuki S, Watanabe Y, Hashimoto S, Kawashima H. Molecular cloning and functional expression of a cDNA encoding the human V_{1b} vasopressin receptor. *J Biol Chem.* 1994;269:27088–27092.
4. Lolait SJ, O'Carroll AM, McBride OW, Konig M, Morel A, Brownstein MJ. Cloning and characterization of a vasopressin V2 receptor and possible link to nephrogenic diabetes insipidus. *Nature.* 1992;357:336–339.
5. Kimura T, Tanizawa O, Mori K, Brownstein MJ, Okayama H. Structure and expression of a human oxytocin receptor. *Nature.* 1992;356:526–529.
6. Lolait SJ, O'Carroll AM, Mahan LC, et al. Extrapituitary expression of the rat V1b vasopressin receptor gene. *Proc Natl Acad Sci USA.* 1995;92:6783–6787.
7. Saito M, Sugimoto T, Tahara A, Kawashima H. Molecular cloning and characterization of rat V1b vasopressin receptor: evidence for its expression in extrapituitary tissues. *Biochem Biophys Res Commun.* 1995;212:751–757.
8. Rabadan-Diehl C, Makara G, Kiss A, et al. Regulation of pituitary V1b vasopressin receptor messenger ribonucleic acid by adrenalectomy and glucocorticoid administration. *Endocrinology.* 1997;138:5189–5194.
9. Scott LV, Dinan TG. Vasopressin and the regulation of hypothalamic-pituitary-adrenal axis function: implications for the pathophysiology of depression. *Life Sci.* 1998;62:1985–1998.
10. Aguilera G, Rabadan-Diehl C. Vasopressinergic regulation of the hypothalamic-pituitary-adrenal axis: implications for stress adaptation. *Regul Pept.* 2000;96:23–29.
11. Griebel G, Simiand J, Serradeil-Le Gal C, et al. Anxiolytic- and antidepressant-like effects of the non-peptide vasopressin V1b receptor antagonist, SSR149415, suggest an innovative approach for the treatment of stress-related disorders. *Proc Natl Acad Sci USA.* 2002;99:6370–6375.
12. Serradeil-Le Gal C, Wagnon J, Simiand J, et al. Characterization of (2S,4R)-1-[5-chloro-1-[(2,4-dimethoxyphenyl)sulfonyl]-3-(2-methoxy-phenyl)-2-oxo-2,3-dihydro-^{1}H-indol-3-yl]-4-hydroxy-N,N-dimethyl-2-pyrrolidine carboxamide (SSR149415), a selective and orally active vasopressin V_{1b} receptor antagonist. *J Pharmacol Exp Ther.* 2002;300:1122–1130.
13. Edwards S, Guerrero M, Ghoneim OM, Roberts E, Koob GF. Evidence that vasopressin V1b receptors mediate the transition to excessive drinking in ethanol-dependent rats. *Addict Biol.* 2012;17:76–85.
14. Iijima M, Yoshimizu T, Shimazaki T, et al. Antidepressant and anxiolytic profiles of newly synthesized arginine vasopressin V_{1B} receptor antagonists: TASP0233278 and TASP0390325. *Br J Pharmacol.* 2014;171:3511–3525.
15. Griebel G, Beeské S, Stahl SM. The vasopressin V_{1b} receptor antagonist SSR149415 in the treatment of major depressive and generalized anxiety disorders:

results from 4 randomized, double-blind, placebo-controlled studies. *J Clin Psychiatry.* 2012;73:1403–1411.
16. Katz DA, Locke C, Liu W, et al. Single-dose interaction study of the arginine vasopressin type 1B receptor antagonist ABT-436 and alcohol in moderate alcohol drinkers. *Alcohol Clin Exp Res.* 2016;40:838–845.
17. Koga K, Yoshinaga M, Uematsu Y, et al. TASP0434299: a novel pyridopyrimidin-4-one derivative as a radioligand for vasopressin V_{1B} receptor. *J Pharmacol Exp Ther.* 2016;357:495–508.
18. Yoshinaga M, Miyakoshi N, Koga K, inventors; Taisho Pharmaceutical Co. Ltd., assignee. Pyridopyrimidin-4-one derivative PCT. Pub. no. WO/2013/191244. December 27, 2013.
19. Koga K, Maeda J, Tokunaga M, et al. Development of TASP0410457 (TASP457), a novel dihydroquinolinone derivative as a PET radioligand for central histamine H_3 receptors. *EJNMMI Res.* 2016;6:11.
20. Lolait SJ, Roper JA, Hazell GGJ, Li Y, Thomson FJ, O'Carroll AM. Neuropeptide receptors. In: Murphy D, Gainer H, eds. *Molecular Neuroendocrinology: From Genome to Physiology.* Hoboken, NJ: John Wiley & Sons, Ltd.; 2016:195–218.
21. Young WS, Li J, Wersinger SR, Palkovits M. The vasopressin 1b receptor is prominent in the hippocampal area CA2 where it is unaffected by restraint stress or adrenalectomy. *Neuroscience.* 2006;143:1031–1039.
22. Roper J, O'Carroll AM, Young WS, Lolait SJ. The vasopressin Avpr1b receptor: Molecular and pharmacological studies. *Stress.* 2011;14:98–115.
23. Innis RB, Cunningham VJ, Delforge J, et al. Consensus nomenclature for in vivo imaging of reversibly binding radioligands. *J Cereb Blood Flow Metab.* 2007;27:1533–1539.
24. Hilton J, Yokoi F, Dannals RF, Ravert HT, Szabo Z, Wong DF. Column-switching HPLC for the analysis of plasma in PET imaging studies. *Nucl Med Biol.* 2000; 27:627–630.
25. Katz DA, Liu W, Locke C, Dutta S, Tracy KA. Clinical safety and hypothalamic-pituitary-adrenal axis effects of the arginine vasopressin type 1B receptor antagonist ABT-436. *Psychopharmacology (Berl).* 2016;233:71–81.
26. Aguilera G, Pham Q, Rabadan-Diehl C. Regulation of pituitary vasopressin receptors during chronic stress: relationship to corticotroph responsiveness. *J Neuroendocrinol.* 1994;6:299–304.